Dieses Dokument ist eine Zweitveröffentlichung (Verlagsversion) /

This is a self-archiving document (published version):

Sandeep Gorantla, Alicja Bachmatiuk, Jeonghyun Hwang, Hussain A. Alsalman, Joon Young Kwak, Thomas Seyller, Jürgen Eckert, Michael G. Spencer, Mark H. Rümmeli

A universal transfer route for graphene

Diese Version ist verfügbar / This version is available on:

https://nbn-resolving.org/urn:nbn:de:bsz:14-qucosa2-362888

SLUB
Wir führen Wissen.

TECHNISCHE
UNIVERSITÄT
DRESDEN

QUCOSA
Quality Content of Saxony

A universal transfer route for graphene†

Sandeep Gorantla,[a] Alicja Bachmatiuk,[bc] Jeonghyun Hwang,[d] Hussain A. Alsalman,[d] Joon Young Kwak,[d] Thomas Seyller,[e] Jürgen Eckert,[af] Michael G. Spencer[e] and Mark H. Rümmeli*[bc]

Often synthetic graphene requires transfer onto an arbitrary substrate prior to use because the substrate it was originally synthesized on is inappropriate for either electrical measurement or characterization. While a variety of routes have been developed they are substrate dependant and often involve the use of harsh treatments. Here we present a facile and cheap route that can be applied to graphene over any substrate. This universal transfer route is based on a wet chemical reaction producing gaseous species which can intercalate between the substrate and the graphene and thus gently delaminate the two.

Introduction

In the current drive to develop efficient routes for high yield, high quality synthetic graphene, the use of chemical vapor deposition (CVD) with metal catalysts dominates. Hence, a key processing requirement for synthetic graphene characterization (*e.g.* examination in a transmission electron microscope (TEM)) or use in applications (*e.g.* graphene based devices) is the ability to transfer it onto arbitrary substrates in a non-destructive fashion. In terms of graphene based applications, the direct growth of graphene on the substrate of need may not be convenient. For example, large area graphene is best grown over metal substrates (*e.g.* Cu, Ni, MoNi) however for electronic device applications graphene is required to reside on a dielectric substrate, thus necessitating transfer.[1] The direct growth of graphene over dielectric substrates such as MgO,[2] SiO$_2$ (ref. 3 and 4) and SiC[5,6] is also possible; however, these techniques are yet to prove themselves for high quality large area growth in an efficient manner. Moreover, even if these synthesis routes are appropriate for direct application integration there is often a

need to transfer them to other supports for characterization, either to better comprehend fundamental growth processes or to characterize the material, for example, the micro/nano-structural characterization of graphene by transmission electron microscopy (TEM).[7–12]

A variety of transfer routes to transfer graphene have been reported, however, these routes are substrate specific and each tends to have its own drawbacks (see Table 1). For example, most transfer routes implemented to transfer graphene off metal surfaces are not suited for transfer off dielectric surfaces. Indeed, graphene transfer off dielectric surfaces is far more difficult than for metal substrates since they are chemically more stable and not easily etched. As a consequence fewer routes exist and they tend to be less straightforward.[6,13,14]

Moreover, most of the methods that do exist to transfer graphene off dielectrics require harsh treatments such as the implementation of strong acids[20–23] or complicated transfer steps *e.g.* the deposition of successive thin films of Au and a polymer over graphene followed by subsequent mechanical peeling.[6] The difficulties encountered in separating graphene from non-metal substrates are primarily because they are more chemically inert as compared to metals and so they are not readily etched.

In this work we demonstrate a novel, facile and damage free transfer route that is suitable to transfer graphene off both metals and non-metals. The transfer route exploits the use of a vigorous bubbling reaction in a solution using commonly available and inexpensive chemicals. The potential of using bubbles to delaminate graphene has previously been demonstrated in electrochemical reactions.[24,25] However, the use of electrochemical reactions is inherently limited in that it requires a conductive substrate and an electro-chemical setup. Our route dispenses with the need for an electro-chemical setup requiring only a bath in which the chemical solutions can be mixed and, at times, gently heated (80 °C). Moreover, any substrate, be it electrically conductive or not, can be used. We demonstrate the universality of the route by transferring

[a] *IFW Dresden, Institute for Complex Materials, PO Box 270116, 01171 Dresden, Germany*

[b] *IBS Center for Integrated Nanostructure Physics, Institute for Basic Science (IBS), Daejon 305-701, Republic of Korea. E-mail: m.ruemmeli@ifw-dresden.de; mhr1@ skku.edu*

[c] *Department of Energy Science, Department of Physics, Sungkyunkwan University, Suwon 440-746, Republic of Korea*

[d] *School of Electrical and Computer Engineering, Cornell University, Ithaca, NY 14853, USA*

[e] *Institute of Physics, Chemnitz University of Technology, 09126 Chemnitz, Germany*

[f] *Institute of Materials Science, Dresden University of Technology, 01062 Dresden, Germany*

Table 1 Selected list of commonly used graphene transfer protocols[a]

Technique	Transfer substrate	Graphene preparation	Advantages	Disadvantages	Reference
Scotch tape	Si/SiO$_2$, SiC	• Mechanically exfoliated HOPG • EG on SiC	Dry transfer from inert substrates	Low yield Residual polymer contamination	15 and 16
PMMA mediated, NaOH + H$_2$O sol	Si/SiO$_2$	• Mechanically exfoliated HOPG	Ease of transfer Preserves initial location of the graphene flakes	Limited to SiO$_2$/Si Polymer removal Residual polymer contamination	17
IPA drop adherence	Si/SiO$_2$, Cu	• Mechanically exfoliated HOPG	No polymer support film Obtain free-standing graphene	Limited to SiO$_2$/Si Need a carbon film on the target substrate Low yield Residual polymer contamination	18 and 19
PMMA/PDMS mediated, metal etching	Cu, Ni	• CVD	Ease of transfer Enables transfer of large area graphene	Limited to substrates that can be easily etched Use of strong acids Nanoparticle metal contamination Residual polymer contamination Longer preparation time	20–23
Electrochemical bubbling	Cu, Ni, Pt	• CVD	No strong acids for etching Beneficial for inert metals Shorter separation time	Needs an electrically conducting substrate Needs an electrochemical cell setup	24 and 25
Mechanical peeling using polymer/Au support layers	SiC, αAl$_2$O$_3$, Si/SiO$_2$	• Epitaxial graphene • CVD • Mechanically exfoliated HOPG	Dry transfer from inert substrates	Complicated multi-step process Need for multiple support layer deposition More defects induced during the transfer process Surface contamination	6, 26 and 27

[a] HOPG: highly oriented pyrolytic graphene; EG: exfoliated graphene; PMMA: polymethyl methacrylate; IPA: isopropyl alcohol; PDMS: polydimethylsiloxane; CVD: chemical vapour deposition.

graphene off Cu, Ni–Mo, Al$_2$O$_3$ and SiC. The graphene is then transferred onto Si/SiO$_2$ wafers or standard perforated carbon film transmission electron microscopy (TEM) grids.

Experimental

PMMA deposition

PMMA (950 K grade, 4 wt% in chlorobenzene, supplier: ALL-RESIST) is spin-coated on the substrates with graphene *via* a 2-step process (step 1: 600 rpm at 10 s and step 2: 1200 rpm for 60 s) using a Laurell® WS-400BZ-6NPP/LITE spin coater. Next, the deposited PMMA is cured at 150 °C for 15 min.

Graphene transfer to TEM grids

After the separation of the PMMA–graphene film from the growth substrate is conducted using our transfer method and subsequent cleaning the film is deposited on lacey/holey carbon coated TEM grids. The DI-water surface tension is used to pull the PMMA–graphene film onto the TEM grid into intimate contact.

The TEM grids with a PMMA–graphene film are air-dried overnight to evaporate any remaining water at the interface between the film and the lacey carbon of the TEM grid. To remove the PMMA, the TEM grids are held with the aid of cross-tweezers on the surface of acetone instead of the conventional approaches of either soaking the TEM grid in acetone solution or exposing the TEM grid to acetone vapour. We observed that contact of the TEM grid through surface tension on the surface of acetone is the optimal solution over the aforementioned conventional approaches to avoid the tearing of the lacey carbon support film and to successfully dissolve away the PMMA in acetone. After the removal of the PMMA, the TEM grids are annealed in vacuum (~10^{-5} mbar) at 120 °C for about 10 hours to evaporate remaining acetone and any other

hydrocarbon contamination on the graphene. Prior to transfer the substrates were rinsed with IPA.

Characterization

Raman spectroscopy was conducted using a Thermo Scientific DXR Raman spectrometer with an excitation laser with $\lambda = 532$ nm. For the Raman characterization the graphene grown on different substrates was transferred onto Si/SiO$_2$. Transmission electron microscopy investigations were carried out at 80 kV accelerating voltage on a JEOL JEM2010F TEM retrofitted with two Cs correctors.[43]

Results and discussion

Our universal graphene transfer route exploits the use of vigorous bubble production through a disproportionation reaction to delaminate graphene that had previously been coated with a thin layer of poly(methyl methacrylate) (PMMA) by spin coating (panel a of Fig. 1). Here the PMMA coating serves as a support/carrier material for the graphene.[28–30] In our transfer method, a solution mixture of NH$_4$OH + H$_2$O$_2$ + H$_2$O (1 : 1 : 3 vol%) is used. This solution mixture is similar to the standard SC1 solution developed by the Radio Corporation America (RCA) for cleaning Si wafers.[31] Henceforth we refer to the NH$_4$OH + H$_2$O$_2$ + H$_2$O (1 : 1 : 3 vol%) solution used in this work as modified-SC1 (MSC1) solution. Upon combining NH$_4$OH + H$_2$O$_2$ + H$_2$O (1 : 1 : 3 vol%) at 80 °C a vigorous bubbling reaction is observed due to the rapid dissociation of H$_2$O$_2$ into H$_2$O and O$_2$ (gas) in the presence of NH$_4$OH which serves as a catalyst for the reaction.

The disproportionation reaction of the H$_2$O$_2$ decomposition, in the absence of a catalyst, can be represented as:

$$2H_2O_2 \text{ (aq)} \rightarrow 2H_2O \text{ (l)} + O_2 \text{ (g)}$$
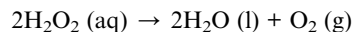
It is worth noting that when transferring graphene off a metal substrate we found that no heating was required as an exothermal catalytic reaction with the metal was sufficient on its own at room temperature.

Once the bubbling process begins the PMMA–graphene/substrate stack is immersed into the solution (panel b of Fig. 1).

During this process one can observe the bubbles to initially seep between the PMMA–graphene film and the substrate interface at the edges. Gradually this process spreads across the interface leading to the eventual detachment of the PMMA–graphene film from the substrate (panel c in Fig. 1). Once the PMMA–graphene film has detached from the substrate it floats to the surface. Thereafter it is fished out and subjected to a 3-stage cleaning procedure (panel d in Fig. 1). In the first cleaning stage the PMMA–graphene film is rinsed with DI water for 20 min by keeping the film afloat on the DI water. In the following step the PMMA–graphene film is transferred onto a fresh solution of MSC1 solution for about 20 min. This step serves as the cleaning step to remove any residual metal/organic contamination on the graphene film. In the final cleaning step, the PMMA–graphene film is again rinsed with distilled water for 20 min. At this stage the PMMA–graphene film can now be transferred onto any desired target substrate (e.g. Si/SiO$_2$ wafer, or perforated carbon film coated TEM grids) as shown in Fig. 1e. Finally, to remove the PMMA from the transferred PMMA–graphene film we have used hot acetone vapour (100 °C) to dissolve away the PMMA as shown in Fig. 1f. This marks the end of our universal graphene transfer route.
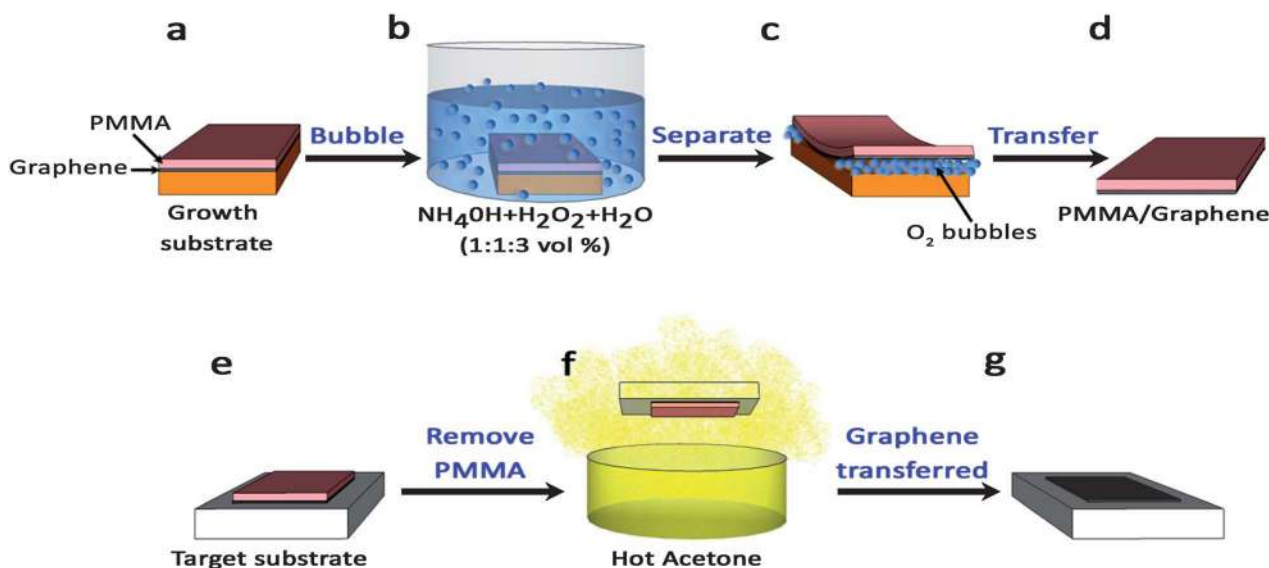

Fig. 1 Schematic of the universal transfer route of graphene over arbitrary substrates. Initially, (a) a PMMA support/carrier layer is deposited on the graphene. (b) The substrate is then transferred into our MSC1 bath in which bubbling due to the release of O$_2$ gas occurs. (c) The O$_2$ gas bubbles intercalate at the graphene–substrate interface leading to (d) gradual detachment of the PMMA–graphene film. (e) The separated film is transferred onto the target substrate and (f) PMMA is removed using hot acetone vapor. (g) This marks the end of successful transfer of graphene onto an arbitrary target substrate.

Transfer of graphene from metal growth substrates

To demonstrate the transfer process of metallic substrates we use CVD grown bi-layer graphene over Cu and monolayer graphene grown over Ni–Mo (similar to the process described by Dai *et al.*[32]). Fig. 2 shows the various stages of our transfer method for CVD grown graphene over copper foil onto a Si/SiO$_2$ substrate. Fig. 2a shows the initial Cu foil with graphene. Fig. 2b shows the same Cu foil after spin coating and curing the PMMA (to ease identification the PMMA film is marked with "P"). The PMMA–graphene/Cu foil stack is then immersed into the MSC1 solution as shown in Fig. 2c and d. Immediately after immersion bubbles begin to appear around the edges of the PMMA–graphene/Cu foil stack as shown in Fig. 2d.

Over a period of *ca.* 30 min, the copper undergoes partial dissolution turning the color of the solution blue and the bubbling becomes even more vigorous (Fig. 2e). The peak bubbling state lasts for 1 to 3 min, after which the bubbling rate decreases and then ceases (Fig. 2f). The reaction leads to the PMMA–graphene film separating from the growth substrate with the Cu film sinking and the PMMA–graphene film floating on the surface of the solution since the PMMA–graphene film is hydrophobic (Fig. 2g). The separated PMMA–graphene film is then washed in a 3-stage cleaning process as described above to wash away any residual substrate material and other contaminants. After cleaning and rinsing the PMMA–graphene film is transferred onto a fresh and clean piece of Si/SiO$_2$ wafer by gently fishing the film floating on the DI water with the Si/SiO$_2$ wafer (Fig. 2h). The wafer with the transferred film is then dried overnight in air. In the final step the PMMA is removed by exposing the PMMA–graphene/target substrate stack to hot acetone vapour. Fig. 2i shows the transferred graphene on the Si/SiO$_2$ wafer after PMMA removal. Fig. 2j shows the cropped image of the boxed region in Fig. 2i in false colour for ease of

viewing. In the same manner we are able to transfer CVD grown mono-layer graphene over Ni–Mo substrates onto Si/SiO$_2$ wafers. To confirm the successful transfer of the graphene onto Si/SiO$_2$ wafers we implemented Raman spectroscopy. The most prominent features observed in the Raman spectrum from graphene are the G mode around 1580 cm^{-1} and the 2D mode which sits around 2700 cm^{-1}. Two further peaks can also be observed, the D mode around 1350 cm^{-1} and the G* mode around 2450 cm^{-1}.[33] These features are easily observed for the transferred CVD grown graphene over Cu (Fig. 3a) and Ni–Mo substrates (Fig. 3b). In the case of the graphene grown over Cu, the 2D mode is slightly wider (FWHM *ca.* 45 cm^{-1}) as compared to monolayer graphene (*ca.* 32 cm^{-1}). In addition, the relative intensity of the 2D to G peaks (1.3 ± 0.1) is less than for monolayer graphene (1.8 ± 0.1). The reduced 2D/G value, and the increase in the FWHM of the 2D mode are concomitant with turbostratic bi-layer graphene, *viz.* AB Bernal stacking is not present or limited.[33,34]

To further demonstrate the versatility of our transfer method we also transferred the CVD grown mono- and bi-layer graphene onto perforated carbon film TEM grids. Fig. 4a and b show the corresponding overview TEM and HRTEM images of bi-layer graphene transferred from Cu foil. Fig. 4b clearly shows the Moiré pattern in the transferred bilayer graphene from Cu due to the rotational stacking.[35] The overview and HRTEM images in Fig. 4c and d further confirm the successful transfer of monolayer graphene from MoNi growth substrates. It is important to note here that in the case of metal growth substrates the MSC1 solution bath was maintained at room temperature without any additional heating. Even at room temperature the bubbling reaction occurs spontaneously a few seconds after immersing the PMMA–graphene/metal substrate stack into the solution. This is because, the metal substrates undergo partial to
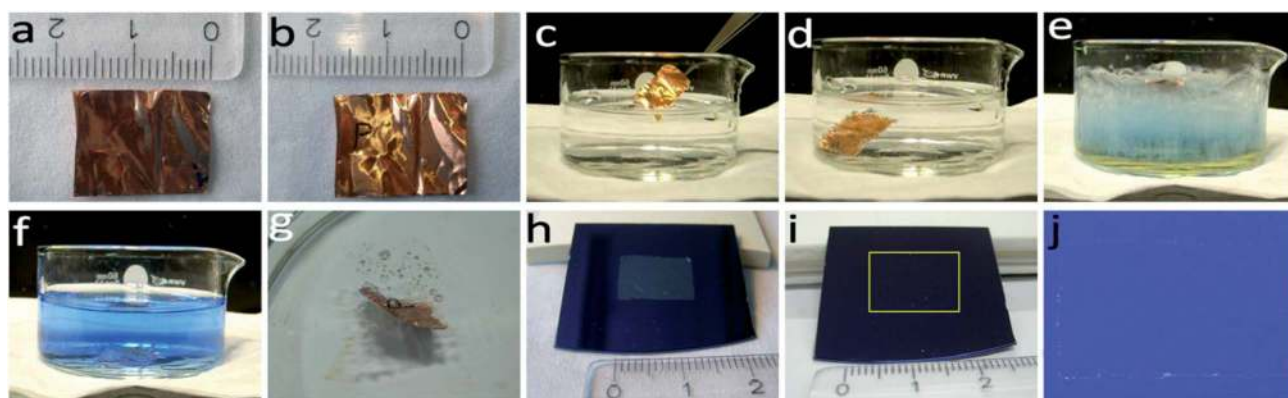

Fig. 2 Critical snapshots of the universal transfer route of CVD grown graphene over Cu foil. (a) The Cu foil with CVD grown graphene. (b) The PMMA film is deposited on this Cu foil and is marked with the letter "P" on the PMMA film. (c) Snapshot showing the immersion of the PMMA–graphene/Cu foil stack into the MSC1 solution. (d) Snapshot of the immersed stack in the solution. (e) Snapshot of the critical bubbling state of the MSC1 solution due to the rapid decomposition of H$_2$O$_2$. The blue coloration of the solution is due to the dissolved Cu^{2+} ions by NH$_4$OH in the MSC1 solution. (f) Critical snapshot showing the MSC1 solution after the complete decomposition of H$_2$O$_2$. (g) Image of the separated PMMA–graphene film (marked P) floating on the surface of DI water and the separated Cu foil immersed in water. (h) The PMMA–graphene film transferred onto a clean Si/SiO$_2$ wafer after overnight air drying. (i) The same Si/SiO$_2$ wafer after removal of the PMMA film using acetone vapour. The transferred graphene on the Si/SiO$_2$ wafer within the highlighted blue yellow boxed region is difficult to see in the photographic image due to weak contrast. (j) Shows the cropped region of the boxed region in false colour clearly showing the transferred graphene (rectangular shaped) on the Si/SiO$_2$ wafer.
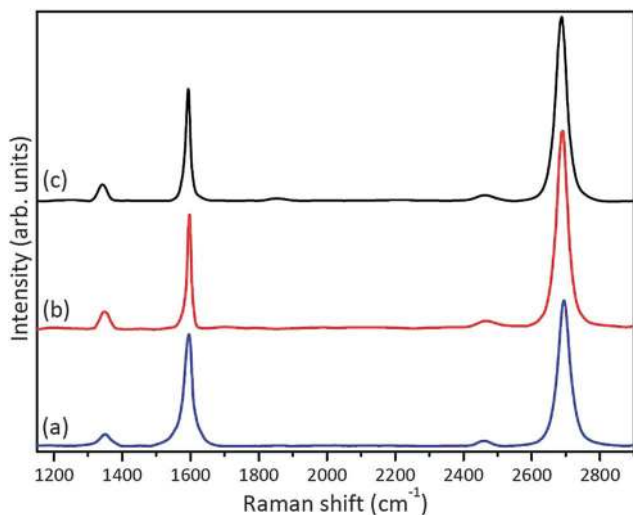
Fig. 3 Raman spectra of the transferred graphene from metal and non-metal growth substrates. The lower spectrum (a) shows the Raman signal from bi-layer graphene transferred from Cu onto a Si/SiO$_2$ wafer and the spectrum in the middle; (b) corresponds to the monolayer graphene transferred from MoNi onto the Si/SiO$_2$ wafer. The upper spectrum (c) corresponds to the monolayer graphene transferred from Al$_2$O$_3$ onto the Si/SiO$_2$ wafer.

complete etching by dissolving through an autocatalytic pathway from the NH$_4$OH in the MSC1 solution.[36] The change in the color of the solution to blue as seen in Fig. 2e when the Cu growth substrate is immersed clearly confirms copper dissolution; it is well known that similar to other amines NH$_4$OH turns blue in the presence of (blue) color Cu^{2+} ions. The decomposition of H$_2$O$_2$ is a thermodynamically favorable process and the rate of decomposition depends on the bath temperature and the presence of impurities that catalyse the decomposition among other factors.[37]

On the other hand the NH$_4$OH can more rapidly decompose dilute hydrogen peroxide in the presence of metal ions, which is the case with our MSC1 solution. In other words, the MSC1 solution spontaneously releases O$_2$ gas causing the vigorous bubbling in the presence of metal graphene growth substrates. This explains why no additional heating of the solution is needed to initiate the formation of bubbles leading to separation of the PMMA–graphene film for the metal growth substrate in our transfer process.

Based on these observations it may be concluded that separation of PMMA–graphene from metal growth substrates in our MSC1 solution may be the result of both the bubbles formed by the release of O$_2$ gas and partial dissolution of the metal substrate in the solution.

The quality of the graphene transferred through our method as compared to the most commonly used transfer route for metals, *i.e.* the PMMA-mediated FeCl$_3$ etching method,[19] was evaluated. For this we compared the Raman spectra of the graphene transferred from the same MoNi substrate onto two different Si/SiO$_2$ wafers using both methods. Fig. S1 in the ESI† shows these comparative Raman spectra. In Fig. S1† the height of the D (defect) mode at *ca.* 1350 cm^{-1} of the lower Raman
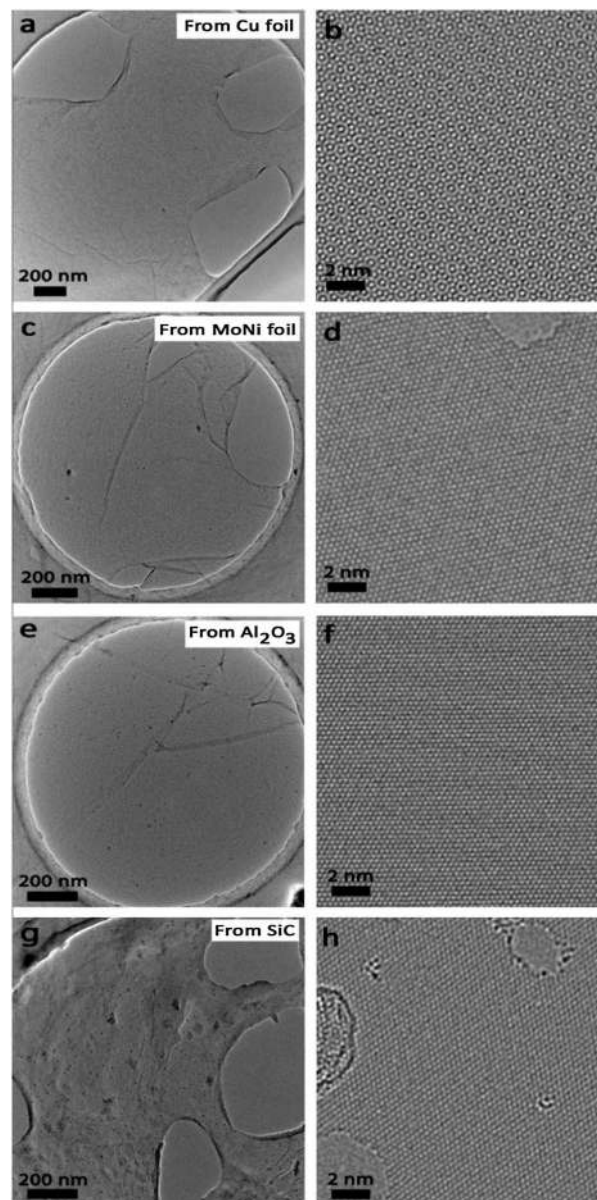

Fig. 4 TEM micrographs of transferred graphene from different arbitrary growth substrates. Panel (a) shows the overview image of bi-layer graphene transferred from a Cu growth substrate. (b) The corresponding HRTEM image of the bi-layer graphene with rotational stacking (note the Moiré pattern indicating a rotational stacking fault). Panels (c) and (d) respectively show the corresponding overview and HRTEM images of monolayer graphene transferred from MoNi. Panels (e) and (f) respectively show the corresponding overview and HRTEM images of monolayer graphene transferred from Si/SiO$_2$ substrates. Panels (g) and (h) respectively show the corresponding overview and HRTEM images of monolayer graphene transferred from Al$_2$O$_3$ respectively. Panels (i) and (j) respectively show the corresponding overview and HRTEM images of monolayer graphene transferred from SiC respectively.

spectrum from the graphene transferred using our method is found to be similar to the height of the D peak in the upper spectrum which corresponds to the graphene transferred through FeCl$_3$. This shows that no damage is caused by our bubbling transfer method.

Transfer of graphene from non-metal growth substrates

More interestingly, as mentioned before, our initial motivation was to transfer graphene grown over Al_2O_3 substrates. Here we show clear evidence that our graphene transfer route can successfully transfer the graphene off various non-metals, namely Al_2O_3 and SiC. The procedure for the transfer from non-metals is the same as in the case of metals as described previously but with one important difference, namely, that the temperature of the MSC1 solution bath has to be maintained at 80 °C for the bubbling reaction to occur. This is probably due to negligible dissolution of the chemically inert non-metal substrates by NH_4OH and, more importantly, the low-catalytic role of such substrates as compared to metals. To demonstrate the potential of our transfer technique we first applied the transfer technique to graphene grown directly over Al_2O_3 by CVD.[38] Initially we transferred the graphene onto a Si/SiO_2 wafer and successfully confirmed the transfer using Raman spectroscopy to identify the presence of graphene on the wafer (see spectrum c in Fig. 3). The Raman spectrum clearly matches that of graphene and confirms its successful transfer by our bubbling technique. We also transferred the graphene to TEM grids successfully as shown in Fig. 4e and f, further confirming the successful transfer of graphene off Al_2O_3. The transfer of graphene from SiC which was grown through the preferential sublimation of Si atoms from the surface of single-crystalline SiC substrates and the subsequent rearrangement of carbon atoms into graphene was also explored using our developed technique.[39–41] In this work, we used SiC substrates with epitaxial graphene grown on the Si-terminated surface where it is known that a significant fraction of C atoms in the graphene lattice is covalently bound to surface Si atoms of the substrate.[42] This is different in the case of graphene grown on arbitrary substrates through CVD where no such covalent bonding of the graphene with the underlying substrate is present. Based on this, it is obvious that the mere deposition of the PMMA polymer support carrier layer and subsequent bubbling process of our transfer method may not be sufficient to separate the as-produced graphene layer off the SiC substrate. Early experiments confirmed that indeed the implementation of our technique was insufficient to decouple as-grown epitaxial graphene off SiC (Si-face). To de-couple the graphene from the SiC we used graphene over SiC (0001) which had first been exposed to a hydrogenation treatment which leads to hydrogen intercalation and the subsequent breaking of Si–C bonds between the graphene and the SiC surface.[42] This type of treated graphene is commonly referred to as quasi-free-standing graphene on H-saturated SiC (0001). Now, upon applying our transfer route to the quasi free standing graphene over SiC we were able to successfully transfer the graphene as shown in Fig. 4g and h. However, in general, we had to repeat the bubbling step of our transfer method to successfully release the film and this may be attributed to the incomplete hydrogenation of Si–C bonds at the SiC–graphene interface in the hydrogenation treatment.

An alternative transfer route for epitaxial (EG) grown on SiC

We also developed an alternative two-step transfer route for epitaxial graphene from SiC substrates which leads to transfer at the first attempt. The first step in the process is an Au based
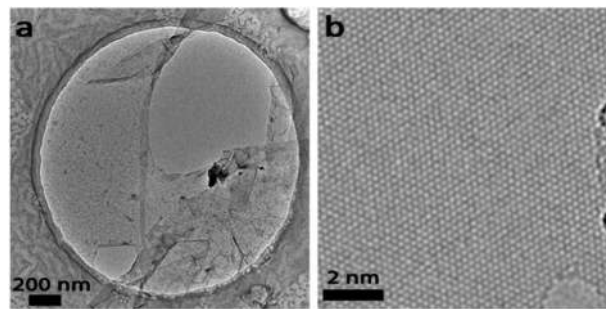

Fig. 5 TEM micrographs of transferred monolayer EG from SiC through an alternative route. Panels (a) and (b) show the overview and HRTEM images, respectively, of monolayer graphene transferred through the alternative route from SiC.

transfer to a Si substrate similar to that reported by Unarunotai et al.[6] The second step in the process utilizes our bubbling approach to transfer the material to a TEM grid. In this demonstration we employ epitaxial graphene formed by sublimation of SiC in atmospheric pressure Ar at 1600 °C. Such graphene has been shown to be much more uniform[5] than the vacuum grown material (usually multi-layer) such as that used in ref. 39. The transfer reported here proceeds as follows: first we deposited 100 nm of Au on the sample by e-beam evaporation followed by spin coating with PMMA. Using sharp tweezers, we mechanically peeled off the graphene/Au/PMMA trilayer and placed it on the Si substrate. PMMA removal is accomplished using acetone, and etching of Au is performed. Using our bubbling method the graphene is then transferred to a TEM grid. The Raman spectra before transfer (on the SiC substrate) and after transfer (onto the Si substrate) confirmed the presence of a monolayer of graphene (see Fig. S2†). In addition, Raman spectra from the SiC substrate after transfer did not show the presence of a graphene signature as shown in Fig. S2a† further confirming the removal of graphene from the SiC surface (Fig. 5).

The delaminating process

In our universal (bubbling) transfer route the key driving force to separate graphene from its underlying substrate is the formation of oxygen bubbles that are able to intercalate at the graphene–substrate interface and provide a gentle force to peel off the PMMA–graphene film. This is similar to the process encountered in the electrochemical delaminating of graphene grown over Cu and Pt foils.[24,25] A key drawback in the electrochemical route is that the substrate must be conductive and so is not appropriate for non-conductive substrates. This highlights a key advantage of our route that the substrate does not need to be conductive. Moreover, no electrochemical set up is needed making the process not only simpler but also cheaper.

Conclusions

We have successfully developed a universal transfer route for graphene that lifts off graphene residing over both metal and

non-metal substrates. Our transfer route takes advantage of the release of O_2 gas in a $NH_4OH + H_2O_2 + H_2O$ (1 : 1 : 3 vol%) solution during which the H_2O_2 decomposes serving as an oxygen source. The produced oxygen is able to intercalate at the substrate–graphene interface providing a gentle peeling force. Our transfer route is attractive in that it minimizes the need for highly aggressive solutions like $FeCl_3$, $Fe(NO_3)_3$ or HF to etch away the growth substrates and this leads to negligible contamination from the substrate material being observed on the transferred graphene. The technique is easy to use, requires minimal equipment and chemicals which are cheap and easily obtained. We anticipate a new family of routes to emerge in the future in which other gas generating chemical reactions are used. Moreover, the basic technique is likely suited to the transfer of other 2D materials (*e.g.* hBN) from arbitrary substrates.

Acknowledgements

Notes and references

1 A. K. Geim and K. S. Novoselov, *Nat. Mater.*, 2007, **6**, 183–191.

2 M. H. Ruemmeli, A. Bachmatiuk, A. Scott, F. Borrnert, J. H. Warner, V. Hoffman, J.-H. Lin, G. Cuniberti and B. Buechner, *ACS Nano*, 2010, **4**, 4206–4210.

3 J. Sun, N. Lindvall, M. T. Cole, T. Wang, T. J. Booth, P. Bøggild, K. B. K. Teo, J. Liu and A. Yurgens, *J. Appl. Phys.*, 2012, **111**, 044103.

4 H. Medina, Y. C. Lin, C. Jin, C. C. Lu, C. H. Yeh, K. P. Huang, K. Suenaga, J. Robertson and P. W. Chiu, *Adv. Funct. Mater.*, 2012, **22**, 2123–2128.

5 K. V. Emtsev, A. Bostwick, K. Horn, J. Jobst, G. L. Kellogg, L. Ley, J. L. McChesney, T. Ohta, S. A. Reshanov, J. Röhrl, E. Rotenberg, A. K. Schmid, D. H. Waldmann, B. Weber and Th. Seyller, *Nat. Mater.*, 2009, **8**, 203–207.

6 S. Unarunotai, Y. Murata, C. E. Chialvo, H. S. Kim, S. MacLaren, N. Mason, I. Petrov and J. A. Rogers, *Appl. Phys. Lett.*, 2009, **95**, 202101.

7 J. C. Meyer, C. Kisielowski, R. Erni, M. D. Rossell, M. F. Crommie and A. Zettl, *Nano Lett.*, 2008, **8**, 3582–3586.

8 J. H. Warner, M. H. Rümmeli, L. Ge, T. Gemming, B. Montanari, N. M. Harrison, B. Büchner and G. A. D. Briggs, *Nat. Nanotechnol.*, 2009, **4**, 500–504.

9 J. H. Warner, F. Schaeffel, M. H. Ruemmeli and B. Buechner, *Chem. Mater.*, 2009, **21**, 2418–2421.

10 F. Banhart, J. Kotakoski and A. V. Krasheninnikov, *ACS Nano*, 2011, **5**, 26–41.

11 P. Y. Huang, C. S. Ruiz-Vargas, A. M. van der Zande, W. S. Whitney, M. P. Levendorf, J. W. Kevek, S. Garg, J. S. Alden, C. J. Hustedt, Y. Zhu, J. Park, P. L. McEuen and D. A. Muller, *Nature*, 2011, **469**, 389–392.

12 A. W. Robertson, A. Bachmatiuk, Y. A. Wu, F. Schäffel, B. Rellinghaus, B. Büchner, M. H. Rümmeli and J. H. Warner, *ACS Nano*, 2011, **5**, 6610–6618.

13 J. D. Caldwell, T. J. Anderson, J. C. Culbertson, G. G. Jernigan, K. D. Hobart, F. J. Kub, M. J. Tadjer, J. L. Tedesco, J. K. Hite, M. A. Mastro, R. L. Myers-Ward, C. R. Eddy, P. M. Campbell and D. K. Gaskill, *ACS Nano*, 2010, **4**, 1108–1114.

14 K. S. Kim, Y. Zhao, H. Jang, S. Y. Lee, J. M. Kim, K. S. Kim, J. H. Ahn, P. Kim, J. Y. Choi and B. H. Hong, *Nature*, 2009, **457**, 706–710.

15 K. S. Novoselov, A. K. Geim, S. V. Morozov, D. Jiang, Y. Zhang, S. V. Dubonos, I. V. Grigorieva and A. A. Firsov, *Science*, 2004, **306**, 666–669.

16 D. S. Lee, C. Riedl, B. Krauss, K. von Klitzing, U. Starke and J. H. Smet, *Nano Lett.*, 2008, **8**, 4320–4325.

17 A. Reina, H. Son, L. Jiao, B. Fan, M. S. Dresselhaus, Z. F. Liu and J. Kong, *J. Phys. Chem. C*, 2008, **112**, 17741–17744.

18 J. C. Meyer, C. O. Girit, M. F. Crommie and A. Zettl, *Appl. Phys. Lett.*, 2008, **92**, 123110.

19 W. Regan, N. Alem, B. Aleman, B. Geng, C. O. Girit, L. Maserati, F. Wang, M. F. Crommie and A. Zettl, *Appl. Phys. Lett.*, 2010, **96**, 113102.

20 X. Li, W. Cai, J. An, S. Kim, J. Nah, D. Yang, R. Piner, A. Velamakanni, I. Jung, E. Tutuc, S. K. Banerjee, L. Colombo and R. S. Ruoff, *Science*, 2009, **324**, 1312–1314.

21 Y. C. Lin, C. Jin, J. C. Lee, S. F. Jen, K. Suenaga and P. W. Chiu, *ACS Nano*, 2011, **5**, 2362–2368.

22 A. Reina, X. Jia, J. Ho, D. Nezich, H. Son, V. Bulovic, M. S. Dresselhaus and J. Kong, *Nano Lett.*, 2009, **9**, 30–35.

23 J. W. Suk, A. Kitt, C. W. Magnuson, Y. Hao, S. Ahmed, J. An, A. K. Swan, B. B. Goldberg and R. S. Ruoff, *ACS Nano*, 2011, **5**, 6916–6924.

24 Y. Wang, Y. Zheng, X. Xu, E. Dubuisson, Q. Bao, J. Lu and K. P. Loh, *ACS Nano*, 2011, **5**, 9927–9933.

25 L. B. Gao, W. Ren, H. Xu, L. Jin, Z. Wang, T. Ma, L. P. Ma, Z. Zhang, Q. Fu, L. M. Peng, X. Bao and H. M. Cheng, *Nat. Commun.*, 2012, **3**, 699, DOI: 10.1038/ncomms1702.

26 H. J. Song, M. Son, C. Park, H. Lim, M. P. Levendorf, A. W. Tsen, J. Park and H. C. Choi, *Nanoscale*, 2012, **4**, 3050–3054.

27 M. Huang, H. Yan, C. Chen, D. Song, T. F. Heinz and J. Hone, *Proc. Natl. Acad. Sci. U. S. A.*, 2009, **106**, 7304–7308.

28 A. Reina, H. Son, L. Jiao, B. Fan, M. S. Dresselhaus, Z. F. Liu and J. Kong, *J. Phys. Chem. C*, 2008, **112**, 17741–17744.

29 X. Li, Y. Zhu, W. Cai, M. Borysiak, B. Han, D. Chen, R. D. Piner, L. Colombo and R. S. Ruoff, *Nano Lett.*, 2009, **9**, 4359–4363.

30 L. Jiao, B. Fan, X. Xian, Z. Wu, J. Zhang and Z. Liu, *J. Am. Chem. Soc.*, 2008, **130**, 12612–12613.

31 *Handbook of Semiconductor Cleaning Technology*, ed. W. Kern, Noyes Publishing, Park Ridge NJ, ch. 1, 1993.

32 B. Dai, L. Fu, Z. Zou, M. Wang, H. Xu, S. Wang and Z. Liu, *Nat. Commun.*, 2011, **2**, 522, DOI: 10.1038/ncomms1539.

33 J. H. Warner, F. Schaeffel, A. Bachmatiuk and M. H. Ruemmeli, *Graphene: Fundamentals and Emerging Applications*, Elsevier, UK, ch. 5.2, 2013.

34 L. M. Mallard, M. A. Pimentaa, G. Dresselhaus and M. S. Dresselhaus, *Phys. Rep.*, 2009, **473**, 51–87.

35 J. H. Warner, M. H. Ruemmeli, T. Gemming, B. Buechner and G. A. D. Briggs, *Nano Lett.*, 2009, **9**, 102–106.

36 B. C.-Y. Lu and W. F. Graydon, *J. Am. Chem. Soc.*, 1977, **77**, 6136–6139.

37 R. H. Petrucci, *General Chemistry: Principles & Modern Applications*, Prentice Hall, 9th edn, 2007, vol. 606.

38 J. Hwang, M. Kim, D. Campbell, H. A. Alsalman, J. Y. Kwak, S. Shivaraman, A. R. Woll, A. K. Singh, R. G. Hennig, S. Gorantla, M. H. Rümmeli and M. G. Spencer, *ACS Nano*, 2013, **7**, 385–395.

39 C. Berger, Z. Song, X. Li, X. Wu, N. Brown, C. Naud, D. Mayou, T. Li, J. Hass, A. N. Marchenkov, E. H. Conrad, P. N. First and W. A. de Heer, *Science*, 2006, **312**, 1191–1196.

40 N. Camara, A. Tiberj, B. Jouault, A. Caboni, B. Jabakhanji, N. Mestres, P. Godignon and J. Camassel, *J. Phys. D: Appl. Phys.*, 2010, **43**, 374011.

41 P. N. First, W. A. de Heer, T. Seyller, C. Berger, J. A. Stroscio and J. S. Moon, *MRS Bull.*, 2010, **35**, 296–305.

42 F. Speck, J. Jobst, F. Fromm, M. Ostler, D. Waldmann, M. Hundhausen, H. B. Weber and T. Seyller, *Appl. Phys. Lett.*, 2011, **99**, 122106.

43 F. Börrnert, A. Bachmatiuk, S. Gorantla, D. Wolf, A. Lubk, B. Büchner and M. H. Rümmeli, *J. Microsc.*, 2013, **249**, 87–92.